

## Location site of lanthanides in ZnO

Otal, E.,<sup>1</sup> Cánepa, H. R.,<sup>1</sup> and Walsoe de Reça, N. E.<sup>1</sup>

<sup>1</sup>Consejo Nacional de Investigaciones Científicas y Técnicas - Buenos Aires Argentina

### INTRODUCTION

Zinc oxide (ZnO) is a well-known wide-band-gap semiconductor material which has applications in UV light emitters [1], ozone sensors [2], cold field electron emitters [3], transparent electrodes[4], and piezoelectric devices[5]. Otherwise rare earth doped nanometric materials acquired an increased interest in the field of optical communication, phosphors, photonic crystals and displays. Recently, erbium-doped ZnO has demonstrated to be a promising material in optical telecommunication applications. Erbium-doped ZnO has been prepared by laser ablation [6], ion implantation [7], electrochemical precipitation [8] and e-beam evaporation [9]. In this project soft chemistry routes [10], were used to obtain nanocrystalline ZnO with erbium as doping element. As properties of doped materials depend on location site of the doping element in host structure, EXAFS measurements were performed in order to obtain this information. Coordination number and neighbors distance can be determined by modeling and fitting of EXAFS signal, whereas site symmetry can be determined by the analysis of the XANES region.

### EXPERIMENT

Rare earth doped nanocrystalline ZnO was obtained by forced hydrolysis (HM) [11] and precipitation in polar aprotic solvent (PM) [12].methods. The doping elements can be introduced into the host matrix or segregated in more stable phases. Samples were obtained from aqueous solutions at temperatures lower than 80 C and in dry solvents to avoid crystal growth. Primary characterizations were obtained by XRD in a conventional X-ray diffractometer. All samples showed crystal size lower than 10 nm. The XAFS experiment were carried out at the D04B-XAFS1 beam line at the LNLS, Campinas, Brazil.

### RESULTS AND DISCUSSION

The radial distribution (Figure 1) shows a peak with a shoulder that can be attributed to the separation of the first shell in two sub-shells (SS). The fitting of this SS gives a first SS with  $d_{Er-O} = 1.78 \text{ \AA}$  and a second SS with  $d_{Er-O} = 2.34 \text{ \AA}$ . The lack of a second shell can be attributed to several reasons: difference in the phase of atoms forming the first and second shell giving a sum equal to zero (paths Er-O-Er and Er-Zn-Er by example), inclusion of Er in ZnO lattice, which can produce a great disorder in the matrix due to larger Er ionic radius ( $Zn=60 \text{ pm}$  and  $Er=89 \text{ pm}$ ) that could destroy the

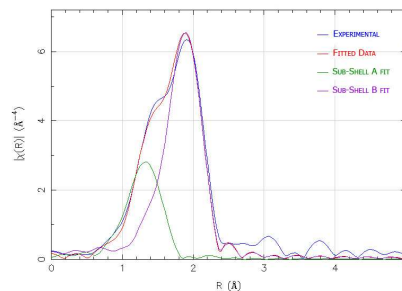


FIG. 1: Fourier transform of  $k^3 \psi$  for ZnO:Er and RSF for two sub shells fitting

signal[13] and finally that Er atoms are located on the surface of ZnO nanoparticles. The SS lost by phase difference was neglected by simulations of that by Feff in Artemis. The hypothesis of a great disorder in the matrix due to larger Er ionic radii destroying the information of second shell is not negligible, in accordance with preliminary results of XANES simulations for Er atoms located in interstitial sites with  $C_{4v}$  distortion. This simulations shows good agreement with experimental data, not only after the white peak region, even the shape of the peak shows good agreement due to the lack of the shoulder shown in figure 2.

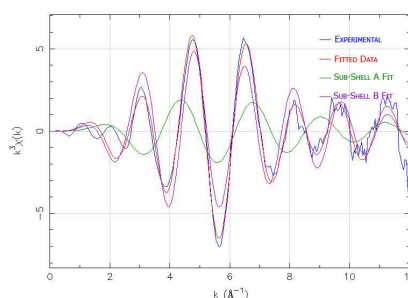


FIG. 2:  $k^3$  weighted XAFS spectra for ZnO:Er and first shell sub shells fitting

XANES simulation were performed using Feff 8.4 code. The inclusion of f-electrons required the modification of this code to increase SCF and FMs and for achieving convergence in calculations. Figure 3 shows the experimental and simulated spectra of  $Er_2 O_3$  with and without shift correction. The energy shift observed in Figure 3 could not be attributed to experimental errors because all the experimental data were corrected using the K-edge of a nickel metallic film (8333 eV).

The inclusion of only one Er atom in interstitial position

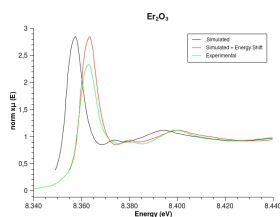


FIG. 3: XANES simulation of  $Er_2O_3$

with octahedral coordination is considered in Figure 4, and the inclusion of two Erbium atoms in the same position, with 2.6Å separation is considered in Figure 5.

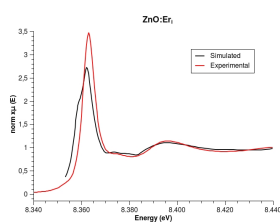


FIG. 4: XANES simulation for  $ZnO:Er_i$

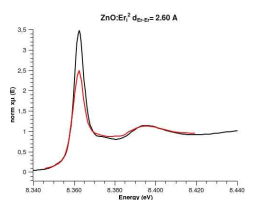


FIG. 5: XANES simulation for  $ZnO:Er_{2i}$

It can be seen clearly in Figure 5 that the shoulder in the simulation with only one atom disappears with the inclusion of the second atom. The effect could be related with lanthanide-lanthanide coupling exchange [14]. Early results of simulations with only one atom and  $C_{4v}$  site symmetry show that this shoulder is not affected by loss of symmetry although, beyond the white pick, signal is slightly changed.

## CONCLUSION

Substitute site can be neglected due to the great differences between experimental data and simulated results. The reason for this fact can be due to larger Er ionic radius. Erbium

atoms can be placed on the surface of nanoparticles due to the nanoparticles have not the same possibilities that bulk materials to relax the strain that implicates the introduction of dopants[15]. Otherwise the preliminary results for XANES simulation of distorted octahedral symmetry for interstitial erbium shows that this is the location of doping elements Two soft chemistry synthetic paths were tested with optimal results to avoid phase segregation. The calculations of coordination number and first shell distances must be done once the occupation site is unique.

## ACKNOWLEDGEMENTS

This work has been supported by the Brazilian Synchrotron Light Laboratory (LNLS) under proposal D04B - XAFS1 6673 and various funding supports provided by CONICET (Argentina), PROSUL (Brazil) and YPF Foundation. We would like to extend our thanks to Dr. Ismael Fábregas and Dr. Gustavo Azevedo for their valuable assistance in data

- [1] Y. Chen, D. M. Bagnall, Z. Zhu, T. Sekiuchi, K. Park, K. Hiraga, T. Yao, S. Koyama, M. Y. Shen and T. Goto: J. Cryst. Growth 181 (1997) 165.
- [2] R. Martins, E. Fortunato, P. Nunes, I. Ferreira and A. Marques: J. Appl. Phys. 96 (2004) 1398.
- [3] C. J. Lee, T. J. Lee, S. C. Lyu and Y. Zhang: Appl. Phys. Lett. 81 (2002) 3648.
- [4] X. Jiang, F. L. Wong, M. K. Fung and S. T. Lee: Appl. Phys. Lett. 83 (2003) 1875.
- [5] S. Komuro, T. Katsumata, T. Morikawa, X. Zhao, H. Isshiki and Y. Aoyagi: J. Appl. Phys. 88 (2000) 7129.
- [6] P. X. Gao and Z. L. Wang: J. Appl. Phys. 97 (2005) 044304.
- [7] E. Rita, E. Alves, U. Wahl, J. G. Correia, T. Monteiro, M. J. Soares, A. Neves and M. Peres: Nucl. Instrum. Methods Phys. Res., Sect. B 242 (2006) 580.
- [8] A. Goux, T. Pauporte and D. Lincot: J. Electroanal. Chem. 587 (2006) 193.
- [9] X. T. Zhang, Y. C. Liu, J. G. Ma, Y. M. Lu, D. Z. Shen, W. Xu, G. Z. Zhong and X. W. Fan: Thin Solid Films 413 (2002) 257.
- [10] R. Martins, E. Fortunato, P. Nunes, I. Ferreira, A. Marquez, M. Bender, N. Katsarakis, V. Cimalla and G. Kiriakidis: J. Appl. Phys. 96, 3 (2004) 1398
- [11] Bao, D., Gu, H., Kuang, A. - Thin Solid Films; 1998; 312 (1-2), pp. 37-39.
- [12] Spanhel, L., Anderson, M. A. - J. Am. Chem. Soc.; 1991; 113(8), pp. 2826-2833.
- [13] Antolloy Frenkel, Personal communication (2008)
- [14] V. S. Mironov, Spectrochimica Acta Part 154 (1998) 1607
- [15] Carlo Segre, Personal communication (2008)